Earth-mass dark-matter haloes as the first structures in the early Universe

J. Diemand*, B. Moore & J. Stadel

Institute for Theoretical Physics, University of Zurich, Winterthurerstrasse 190, CH-8057 Zürich, Switzerland

* Present address: Department of Astronomy and Astrophysics, University of California, 1156 High Street, Santa Cruz, California 95064, USA

The Universe was nearly smooth and homogeneous before a redshift of $z = 100$, about 20 million years after the Big Bang[1]. After this epoch, the tiny fluctuations imprinted upon the matter distribution during the initial expansion began to collapse because of gravity. The properties of these fluctuations depend on the unknown nature of dark matter[2–4], the determination of which is one of the biggest challenges in present-day science[5–7]. Here we report supercomputer simulations of the concordance cosmological model, which assumes neutralino dark matter (at present the preferred candidate), and find that the first objects to form are numerous Earth-mass dark-matter haloes about as large as the Solar System. They are stable against gravitational disruption, even within the central regions of the Milky Way. We expect over 10^{15} to survive within the Galactic halo, with one passing through the Solar System every few thousand years. The nearest structures should be among the brightest sources of γ-rays (from particle–particle annihilation).

The cosmological parameters of our Universe and initial conditions for structure formation have recently been measured via a combination of observations, including the cosmic microwave background (CMB)[8], distant supernovae[9,10] and the large-scale distribution of galaxies[11]. Cosmologists now face the outstanding problem of understanding the origin of structure in the Universe from its strange mix of particles and vacuum energy[12,13].

Most of the mass of the Universe must be made up of a kind of non-baryonic particle[1,14] that remains undetected in laboratory experiments. The leading candidate for this 'dark matter' is the neutralino, the lightest supersymmetric particle, which is predicted to solve several key problems in the standard model for particle physics[5]. This cold dark matter (CDM) candidate is not completely collisionless. It can collide with baryons, thus revealing its presence in laboratory detectors, although the cross-section for this interaction is extremely small. In a cubic-metre detector containing $\sim 10^{30}$ baryon particles, only a few collisions per day are expected from the $\sim 10^{13}$ dark-matter particles that flow through the experiment as the Earth moves through the Galaxy. The neutralino is its own anti-particle, and can self-annihilate, creating a shower of new particles including γ-rays[5]. The annihilation rate increases as the density squared; the central regions of the Galaxy and its satellites will therefore give the strongest signal[15–18]. However, the expected rate is very low—the flux of photons on Earth is the same as we would receive from a single candle placed on Pluto. Numerous experiments using these effects are under way that may detect the neutralino within the next decade[7]. Furthermore, in the next few years the Large Hadron Collider (LHC) at CERN will confirm or rule out the concepts of supersymmetry (SUSY)[6].

We followed the growth and subsequent gravitational collapse and virialization of the first structures in the CDM Universe with supercomputer calculations. The challenge is accurately to follow the evolution of the Universe on scales that are many orders of magnitude smaller than previously studied, while also capturing the gravitational dynamics from large scales. We use a multiscale technique[19] to achieve the desired resolution within a small average-density patch of the Universe that is nested within a hierarchy of larger and lower resolution grids of particles.

The fluctuations are imposed on the particles using accurate calculations of the linear theory power spectrum for a SUSY model with a particle mass $m_\nu = 100$ GeV. This includes collisional damping, free streaming and the transfer of fluctuations through the matter-radiation era of the Universe[2–4]. The resulting power spectrum is close to a power law of $P(k) \propto k^n$ with $n = -3$, with an exponential cut-off at 0.6 co-moving parsecs, which corresponds to a mass scale of $10^{-6} M_\odot$, where $M_\odot$ is the mass of the Sun. The cut-off scale depends on the neutralino mass and decoupling energy. From accelerator searches we know that $m_\nu > 37$ GeV and that the cosmic matter density sets an upper limit at 500 GeV. The damping scale for the allowed neutralino models differ from the model we used by less than a factor of three in mass[2–4] and structure formation is therefore very similar in all SUSY-CDM scenarios. A less popular CDM candidate is the axion, which has a much smaller damping scale of $10^{-13} M_\odot$. For comparison we simulated the high-resolution region with an axion CDM fluctuation spectrum on the resolved scales. Both models produce equal halo abundances above $5 \times 10^{-6} M_\odot$, but the axion model also forms bound structures down to the smallest resolved scales; see Fig. 3. Here we concentrate on the properties of the first structures to form in the SUSY-CDM model.

We evolve the initial particle distribution using a parallel multi-stepping tree code, starting at a redshift of $z = 350$ when the fluctuations are still linear. The high-resolution region forms the first nonlinear structures at $z = 60$ and the entire region quickly becomes distorted by the complex tidal field from the surrounding overdensities. By a redshift of $z = 26$, the high-resolution region begins to merge into the lower-resolution surroundings and we do not analyse the region further—however, this is sufficiently late that about 5% of the mass in the region has collapsed into bound dense structures (haloes); see Fig. 1.

The first dark-matter haloes to collapse and virialize are smooth triaxial objects of mass $10^{-6} M_\odot$ and half-mass radii of 10^{-2} pc. Figure 2 shows the density profiles of three representative haloes at $z = 26$ that are well fitted by single power-law density profiles $\rho(r) \propto r^{-\gamma}$ with slopes γ in the range from 1.5 to 2, similar to galactic haloes shortly after their formation[20]. We note that the densities at the virial radius are about an order of magnitude higher than the density at $0.01 r_{\rm virial}$ in a galactic halo today, which makes the survival of many of these haloes as galactic substructure possible. The central resolved densities reach 10^9 times the mean background density at 1% of their virial radii. Unlike galactic and cluster-mass CDM haloes, they do not contain substructure because no smaller-mass haloes have collapsed in the hierarchy.

Figure 3 shows the mass function of haloes. We use a 'friends of friends' algorithm with a linking length set to identify the dense central regions of collapsed haloes, then for each halo centre we recursively search for the radius r_{200} that is at an overdensity of 200 times the cosmic mean density. The resulting halo mass function is steep: $\mathrm{d}n(M)/\mathrm{d}\log M \propto M^{-1}$. For comparison we plot an extrapolation of the halo mass function found on much larger scales $> 10^7 M_\odot$ (ref. 21), which fits surprisingly well up to the cut-off scale of $10^{-6} M_\odot$, below which we find no more structures.

At these epochs the baryons are kept sufficiently warm by the CMB that they are unable to cool and form visible objects such as stars or planets within such tiny systems[13]. The dark haloes may be detected via gravitational effects such as lensing or dynamical perturbations. Although we cannot simulate the entire galactic halo at the resolution required to determine the survival statistics of these objects, we can make some simple estimates of their survival and abundances. As the Galactic halo is assembled, these first objects merge successively into more massive systems. From scales of $10^7 M_\odot$ to $10^{15} M_\odot$ the mass function of substructure is a self-similar power law of slope $\mathrm{d}n(m)/\mathrm{d}m \propto m^{-1.9}$ (ref. 22). Extra-

polating the subhalo mass function to the smallest scales gives us a total number of substructure haloes $N(M > 10^{-6}M_{\odot}) \approx 5 \times 10^{15}$ and the expected number density of subhaloes at the solar radius is $n(R_{\odot}) \approx 500\,\mathrm{pc}^{-3}$, assuming that they trace the mass. Although this extrapolation is made to much smaller masses than simulated previously, the substructure within haloes collapsing at $z \approx 15$ with masses $\sim 10^{7}M_{\odot}$ fits the extrapolation from larger mass scales[23], even though they form from regions of the CDM power spectra with effective index $n \approx -2.95$.

Can these structures survive the strong disruptive gravitational forces from the Galaxy? The tidal radius is simply the inner Lagrange point of the rotation of the two-body system. For haloes with power-law density profiles $\rho(r) \propto r^{-2}$ we find $r_{\mathrm{t}} = (Rv_{\mathrm{sat}})/(\sqrt{2}V_{\mathrm{parent}})$ where v_{sat} and V_{parent} are the effective circular velocities ($V = \sqrt{GM/r}$) of the satellite and main halo, R is the pericentric distance of the satellite and G is the gravitational constant. For the smallest mini-haloes $v_{\mathrm{sat}} \approx 1\,\mathrm{m\,s}^{-1}$ and $r_{200} = 0.01\,\mathrm{pc}$. Therefore, within the Galactic potential these haloes could survive completely intact to about 3 kpc from the centre, well within the galacto-centric position of the Sun. Encounters between haloes and with stars and molecular clouds may disrupt a small fraction of these structures, but using the impulsive heating approximation, we estimate that most will survive with little mass loss.

A significant fraction of the mass may lie within bound structures at our location within the Galaxy, lowering the available smoothly distributed matter necessary for direct detection experiments. The Earth passes through a dark-matter mini-halo every 10,000 years, an encounter which lasts for about 50 years, so that most of the time the Earth is within an underdense region of dark matter. Integrating the mass function from $10^{-6}M_{\odot}$ to $10^{10}M_{\odot}$, normalized such that 10% of the mass is within the substructure above a mass scale of $10^{7}M_{\odot}$ (as given by simulations of Galactic haloes), we find that about 50% of the mass is bound to dark-matter substructures. The velocity perturbation to a planetary orbit or satellite is very small ($\sim 10^{-6}\,\mathrm{m\,s}^{-1}$), well below the observational constraints. However, resonant encounters and the cumulative effects of about 10^{6} impulsive encounters may cause significant perturbations to some of the bodies orbiting in the Oort cloud surrounding the Solar System.

Compact objects in the mass range considered here could produce a microlensing signal in a multiply lensed quasar image, such as time-varying flux differences[24]. The lensing object needs to be smaller than the Einstein radius (in centimetres):

$$r_{\mathrm{E}} = 3.7 \times 10^{16} \sqrt{\frac{M}{hM_{\odot}}} \qquad (1)$$

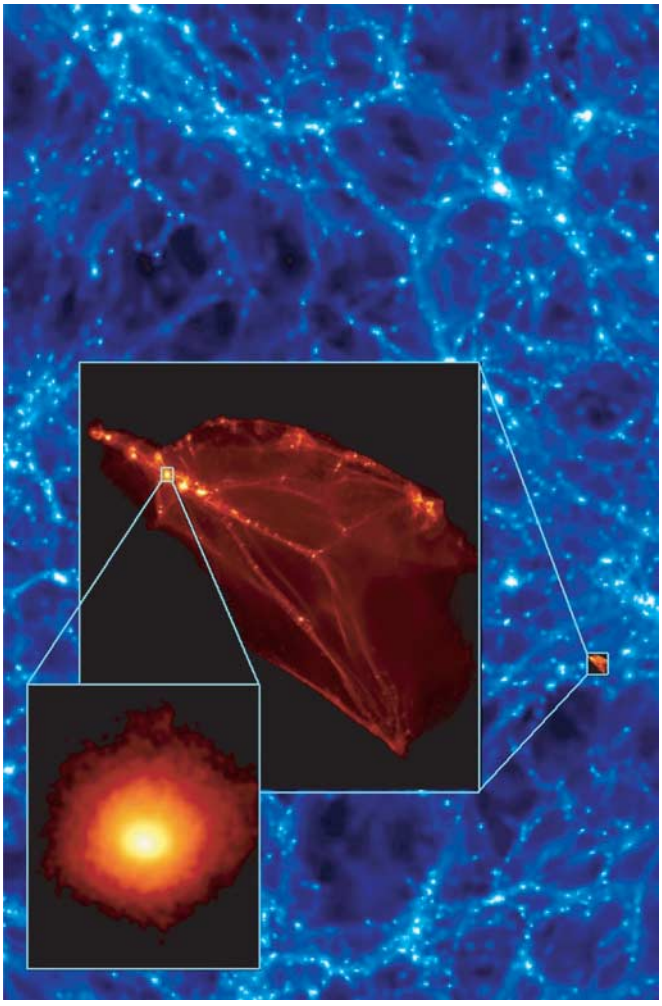

Figure 1 A zoom into one of the first objects to form in the Universe. The colours show the density of dark matter at redshift $z = 26$. Brighter colours correspond to regions of higher concentrations of matter. The blue background image shows the small-scale structure in the top cube (cube size = [3 co-moving kpc]^3) which has a filamentary topology similar to the large-scale structure in the CDM Universe. The first red image zooms by a factor of one hundred into the average-density high-resolution region. This region was initially a cube of 60 co-moving pc^3 resolved with 64 million particles with a gravitational softening of 10^{-2} co-moving parsecs and masses $1.2 \times 10^{-10}M_{\odot} \equiv M_{\mathrm{moon}}/300$. The final image shows a close-up of one of the individual dark-matter haloes in this region, again zooming in by a factor of one hundred so that the box has a physical length of 0.024 pc. This tiny triaxial Earth-mass halo has a central cusp-like density profile and is smooth, devoid of the substructure that is found within galactic and cluster-mass dark-matter haloes. Even though the index of the power spectrum is very steep on these scales ($n \approx -3$), we find that haloes can collapse before merging into a larger system, rather than the naive expectation that all scales are collapsing simultaneously and thus erasing such structures.

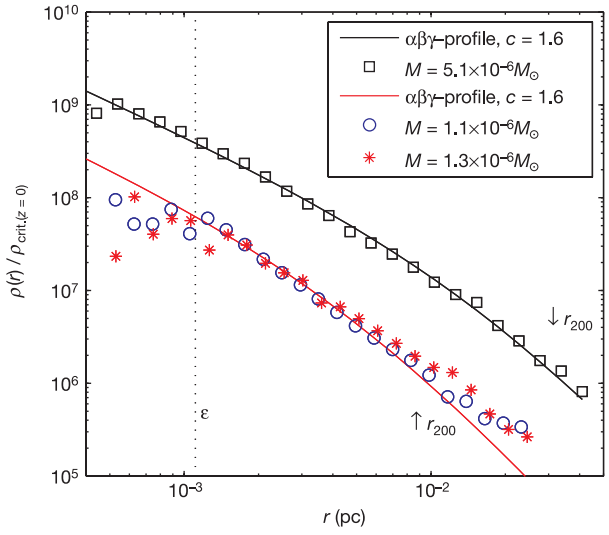

Figure 2 Radial density profiles of three typical minihaloes at redshift $z = 26$. The radial distance is plotted in physical units and we show low-concentration $\alpha\beta\gamma$-profiles for comparison. We use the mean dark-matter profile inferred from the highest-resolution galaxy-cluster simulations[30], that is, $(\alpha\beta\gamma) = (1, 3, 1.2)$. The vertical dotted line indicates our force resolution and the arrows indicate the radii where the halo density is of 200 times the background density. Across the entire range of halo masses from $10^{-6}M_{\odot}$ to $10^{1}M_{\odot}$, we find small concentration parameters $c < 3$. We do not observe a trend of concentration with mass, possibly because the haloes all form at a similar epoch, as expected when the power spectrum is so steep.

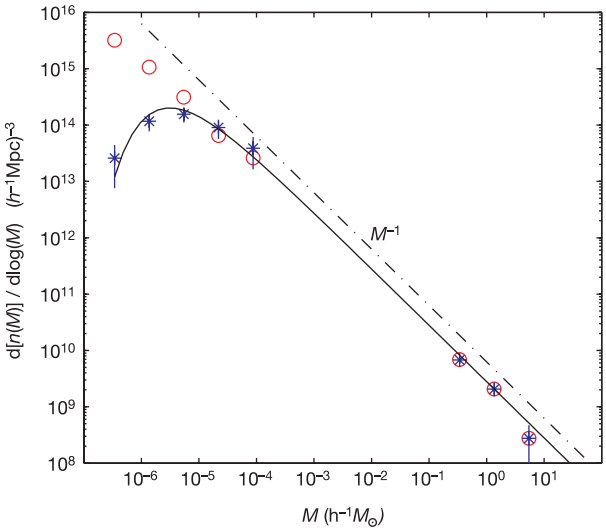

Figure 3 The abundance of collapsed and virialized dark-matter haloes of a given mass. The same region was simulated twice using different types of initial fluctuations: (1) SUSY-CDM with a 100-GeV neutralino (star symbols with 1-σ error bars); and (2) an additional model with no small-scale cut-off to the power spectrum (open circles) as might be produced by an axion dark-matter candidate. Densities are given in co-moving units. Model 2 has a steep mass function down to the resolution limit, whereas run 1 has many fewer haloes below a mass of about $5 \times 10^{-6} h^{-1} M_{\odot} = 3.5 \times 10^{-6} M_{\odot}$, where $h = 0.71$ is the normalized present-day Hubble expansion rate. (Our simulations do not probe the mass range from about $3 \times 10^{-4} h^{-1} M_{\odot}$ to $2 \times 10^{-1} h^{-1} M_{\odot}$). The dashed-dotted line shows an extrapolation of the number density of Galaxy haloes (from ref. 21) assuming $dn(M)/d\log M \propto M^{-1}$. The solid line is the function $dn(M)/d\log M = 2.8 \times 10^{9} (M/h^{-1} M_{\odot})^{-1} \exp[-(M/M_{\mathrm{cut-off}})^{-2/3}]$ in units of $(h^{-1} M\,\mathrm{pc})^{-3}$, with a cut-off mass $M_{\mathrm{cut-off}} = 5.7 \times 10^{-6} h^{-1} M_{\odot}$. The power spectrum cut-off is $P(k) \propto \exp[-(k/k_{\mathrm{fs}})^2]$, where k_{fs} is the free streaming scale and assuming $k \propto M^{-1/3}$ motivates the exponent of $-2/3$ in our fitting function.

For a $10^{-6} M_{\odot}$ object $r_{\mathrm{E}} \simeq 10^{-7}$ pc, which is much smaller than the size of the mini-haloes considered here, so it is unlikely that gravitational lensing can provide a constraint on their presence, either in our halo or on cosmological path lengths to distant quasars.

Indirect detection is a more interesting possibility and several ongoing and planned experiments aim to detect the atmospheric Cerenkov light from γ-rays produced by neutralino annihilation in the cores of dark haloes[7,25–28]. Simple scaling arguments show that minihaloes can have high relative luminosities in γ-rays. The absolute γ-ray luminosity of a dark-matter halo with a Navarro–Frenk–White (NFW) density profile is $L \propto \rho_{\mathrm{s}}^2 r_{\mathrm{s}}^3$, where r_{s} is the scale radius of the NFW profile and $\rho_{\mathrm{s}} = \rho(r_{\mathrm{s}})$ (ref. 29). The relative luminosity that would arrive at the detector from a halo at a distance d is then $L_{\mathrm{rel}} \propto L d^{-2}$.

Now we compare the relative luminosity of a minihalo at a distance of 0.1 pc (their expected mean separation) to the signal from the centre of the Draco dwarf galaxy:

$$\frac{L_{\mathrm{rel,mini}}}{L_{\mathrm{rel,draco}}} \propto \left(\frac{7 \times 10^{6} \rho_{\mathrm{crit}}}{1.7 \times 10^{5} \rho_{\mathrm{crit}}}\right)^{2} \left(\frac{0.005\,\mathrm{pc}}{300\,\mathrm{pc}}\right)^{3} \left(\frac{0.1\,\mathrm{pc}}{82,000\,\mathrm{pc}}\right)^{-1} \approx 5 \quad (2)$$

where we used the typical minihalo properties from our simulations and where ρ_{crit} is the critical energy density. The large abundance of the smallest subclumps compensates their smaller absolute luminosity and the closest of them will be bright sources of γ-rays. The background flux will be enhanced by a boost factor of over two orders of magnitude over a smooth Galactic dark-matter potential. Current indirect detection experiments such as VERITAS[26], HESS[27], MAGIC[28] or CANGAROO-III[25] can probe part of the parameter space predicted by SUSY theory by observing the galactic centre. However this region is dynamically complex because it contains numerous confusing astrophysical γ-ray sources and a supermassive black hole that can erase the central cusp. CDM minihaloes are potentially bright and will not suffer from these problems. All-sky surveys could detect some nearby minihaloes that would have a characteristic extent on the sky, similar to the extent expected for a more distant satellite galaxy like Draco. □

Received 7 September; accepted 3 December 2004; doi:10.1038/nature03270.

1. Peebles, P. J. E. Large-scale background temperature and mass fluctuations due to scale-invariant primeval perturbations. *Astrophys. J.* **263,** L1–L5 (1982).
2. Hofmann, S., Schwarz, D. J. & Stöcker, H. Damping scales of neutralino cold dark matter. *Phys. Rev. D* **64,** 083507 (2001).
3. Berezinsky, V., Dokuchaev, V. & Eroshenko, Y. Small-scale clumps in the galactic halo and dark matter annihilation. *Phys. Rev. D* **68,** 103003 (2003).
4. Green, A. M., Hofmann, S. & Schwarz, D. J. The power spectrum of SUSY-CDM on sub-galactic scales. *Mon. Not. R. Astron. Soc.* **353,** L23–L27 (2004).
5. Jungman, G., Kamionkowski, M. & Griest, K. Supersymmetric dark matter. *Phys. Rep.* **267,** 195–373 (1996).
6. Ellis, J. R., Olive, K. A. & Santoso, Y. Constraining supersymmetry. *New J. Phys.* **4,** 32 (2002).
7. Bertone, G., Hooper, D. & Silk, J. Particle dark matter: Evidence, candidates and constraints. Preprint at ⟨http://arXiv.org/astro-ph/0404175⟩, (2004).
8. Spergel, D. N. *et al.* First-year Wilkinson Microwave Anisotropy Probe (WMAP) observations: Determination of cosmological parameters. *Astrophys. J. Suppl.* **148,** 175–194 (2003).
9. Riess, A. G. *et al.* Observational evidence from supernovae for an accelerating universe and a cosmological constant. *Astron. J.* **116,** 1009–1038 (1998).
10. Perlmutter, S. *et al.* Measurements of omega and lambda from 42 high-redshift supernovae. *Astrophys. J.* **517,** 565–586 (1999).
11. Tegmark, M. *et al.* Cosmological parameters from SDSS and WMAP. *Phys. Rev. D* **69,** 103501 (2004).
12. Peebles, P. J. E. Dark matter and the origin of galaxies and globular star clusters. *Astrophys. J.* **277,** 470–477 (1984).
13. Tegmark, M. *et al.* How small were the first cosmological objects? *Astrophys. J.* **474,** 1–12 (1997).
14. Turner, M. The case for omega mass = 0.33 + /−0.035. *Astrophys. J.* **576,** L101–L104 (2002).
15. Lake, G. Detectability of gamma-rays from clumps of dark matter. *Nature* **346,** 39–40 (1990).
16. Bergstrom, L., Edsjo, J., Gondolo, P. & Ullio, P. Clumpy neutralino dark matter. *Phys. Rev. D* **59,** 043506 (1999).
17. Calcáneo-Roldán, C. & Moore, B. Surface brightness of dark matter: Unique signatures of neutralino annihilation in the galactic halo. *Phys. Rev. D* **62,** 123005 (2000).
18. Prada, F., Klypin, A., Flix, J., Martinez, M. & Simonneau, E. Astrophysical inputs on the SUSY dark matter annihilation detectability. Preprint at ⟨http://arXiv.org/astro-ph/0401512⟩, (2004).
19. Bertschinger, E. Multiscale gaussian random fields at their application to cosmological simulations. *Astrophys. J. Suppl.* **137,** 1–20 (2001).
20. Tasitsiomi, A., Kravtsov, A. V., Gottlober, S. & Klypin, A. A. Density profiles of LCDM clusters. *Astrophys. J.* **607,** 125–139 (2004).
21. Reed, D. *et al.* Evolution of the mass function of dark matter haloes. *Mon. Not. R. Astron. Soc.* **346,** 565–572 (2003).
22. Diemand, J., Moore, B. & Stadel, J. Velocity and spatial biases in cold dark matter subhalo distributions. *Mon. Not. R. Astron. Soc.* **352,** 535–546 (2004).
23. Moore, B. *et al.* Dark matter in Draco and the Local Group: Implications for direct detection experiments. *Phys. Rev. D* **64,** 063508 (2001).
24. Schmidt, R. & Wambsganss, J. Limits on MACHOs from microlensing in the double quasar Q0957+561. *Astron. Astrophys.* **335,** 379–387 (1998).
25. Mori, M. *et al.* (The CANGAROO Collaboration). Status of the CANGAROO-III project. *AIP Conf. Proc.* **558,** 578–581 (2001).
26. Cogan, P. *et al* (The VERITAS Collaboration). An overview of the VERITAS prototype telescope and camera. Preprint at ⟨http://arXiv.org/astro-ph/0408155⟩, (2004).
27. Hinton, J. A. *et al.* (The HESS Collaboration). The status of the HESS project. *New Astron. Rev.* **48,** 331–337 (2004).
28. Cortina, J. *et al.* (The MAGIC Collaboration). Status and first results of the MAGIC telescope. Preprint at ⟨http://arXiv.org/astro-ph/0407475⟩, (2004).
29. Koushiappas, S. M., Zentner, A. R. & Walker, T. P. Observability of gamma rays from neutralino annihilations in the Milky Way substructure. *Phys. Rev. D* **69,** 043501 (2004).
30. Diemand, J., Moore, B. & Stadel, J. Convergence and scatter of cluster density profiles. *Mon. Not. R. Astron. Soc.* **353,** 624–632 (2004).

Acknowledgements We thank A. Green, D. Schwarz, P. Jetzer, M. Miranda, A. Maccio and G. Bertone for discussions. All computations were performed on the zBox supercomputer at the University of Zurich. This work was supported by the Swiss National Science Foundation.

Competing interests statement The authors declare that they have no competing financial interests.

Correspondence and requests for materials should be addressed to B.M. (moore@physik.unizh.ch).